

Supporting Information for:

Salt-Specific Effects in Aqueous Dispersions of Carbon Nanotubes

Manaswee Suttipong,^a Naga Rajesh Tummala,^b and Alberto Striolo^{a,*}

Carlos Silvera Batista^c and Jeffrey Fagan^c

^a School of Chemical, Biological and Materials Engineering, The University of Oklahoma, Norman, Oklahoma 73019–1004

^b School of Chemistry and Biochemistry, Georgia Institute of Technology, Atlanta, Georgia 30332–0400

^c National Institute of Standards and Technology, Materials Science and Engineering Division, Gaithersburg, MD 20899

1. Computational Model

The simulation package GROMACS, version 4.0.7,¹ was employed to study the aggregate morphology of aqueous CsDS surfactants at contact with single-walled carbon nanotubes (SWCNTs). Three SWCNTs, (6,6), (12,12) and (20,20), with diameters of 0.814, 1.628, and 2.713 nm, respectively, were considered. The diameters are obtained as the center-to-center distance between carbon atoms. The SWCNTs were empty, and effectively treated as infinitely long because of periodic boundary conditions. Water molecules, ions, and surfactants were not allowed to enter the SWCNTs.

Within SWCNTs, the carbon atoms were treated as uncharged Lennard-Jones (LJ) spheres and maintained fixed throughout the course of the simulations. The LJ parameters used to describe carbon-carbon interactions were those of Cheng and Steele.²

Water molecules were modeled using the simple point charge extended (SPC/E) model.³

SDS and CsDS molecules were assumed to completely dissociate into dodecyl sulfate ion and Na⁺ or Cs⁺ counter-ion. The parameters for dodecyl sulfate ion were borrowed from those for SDS as described in Ref. 22 and 23. Cs⁺ ions were modeled as proposed by Smith and Dang,⁴ although ions polarizability was not considered. Other details regarding the force field used in our simulations are reported in Ref. 32.

The equations of motion were integrated with a time step of 0.002 ps using the leapfrog algorithm.⁵ The simulations were conducted within the canonical ensemble in which the number of particles (N), the simulation box volume (V), and the temperature (T) were kept constant. All simulations were carried out at 300 K using the Nose-Hoover thermostat with a relaxation time constant of 0.1 ps.⁶ The long-range electrostatic interactions were handled with the particle mesh Ewald method with a precision 10⁻⁴.⁷ The van der Waals interactions were treated with a switching cut-off starting at 8 Å and ending at 10 Å. Note that the non-bond van der Waals

interactions are calculated to cut-off distance and interactions beyond this distance are ignored. The trajectories and velocities were saved every 1000 steps (2 ps) for subsequent analysis.

2. Simulated System

One SWCNT was maintained at the center of one simulation box of dimensions $7.00 \times 7.00 \times 6.1487 \text{ nm}^3$. The cylindrical axis of the SWCNT was aligned along the Z direction of the simulation box and maintained fixed during the simulations. To construct the initial configuration for the systems containing CsDS water and SWCNTs, we used the final configurations obtained from our prior simulations for the correspondent SDS systems,³⁸ but the sodium (Na^+) ions were substituted by Cs^+ ions. When configurations for the SDS systems were not available [i.e., 0.44 and 0.25 $\text{nm}^2/\text{headgroup}$ on (12,12) and (20,20) SWCNTs], we generated initial configurations by first setting the nanotube at the center of the simulation box and then inserting dodecyl sulfate surfactants perpendicularly to the nanotube axis. The Cs^+ and Na^+ ions were randomly placed in the simulation box. The number of water molecules in the box was adjusted to reproduce bulk liquid water density at ambient conditions. Periodic boundary conditions were applied in X, Y, and Z dimensions.

All simulations for CsDS and SDS surfactants on (6,6) SNWTs were conducted for 100 ns. In case of SDS surfactants, we employed final configurations from our previous work³⁸ and further increased the simulation time to 100 ns. For surfactants on (12,12) and (20,20) SWCNTs, the systems were equilibrated for 200 ns. Each system was considered equilibrated because the results did not change during the last 40 ns of the simulations. The trajectories from last 20 ns were used for data analysis.

Details regarding the composition of each simulated systems, including the SWCNTs type, the total numbers of CsDS and water molecules, and nominal surfactant surface coverages are reported in Table S1.

Table S1. Simulation details for the various systems considered.

SWCNT	Number of CsDS molecules	Nominal CsDS surface coverage ($\text{nm}^2/\text{headgroup}$)
(6,6)	19	0.98
(6,6)	36	0.44
(6,6)	64	0.25
(12,12)	71	0.44
(12,12)	126	0.25
(20,20)	119	0.44
(20,20)	210	0.25

3. SDS Surfactants Adsorbed on (6,6) SWCNTs

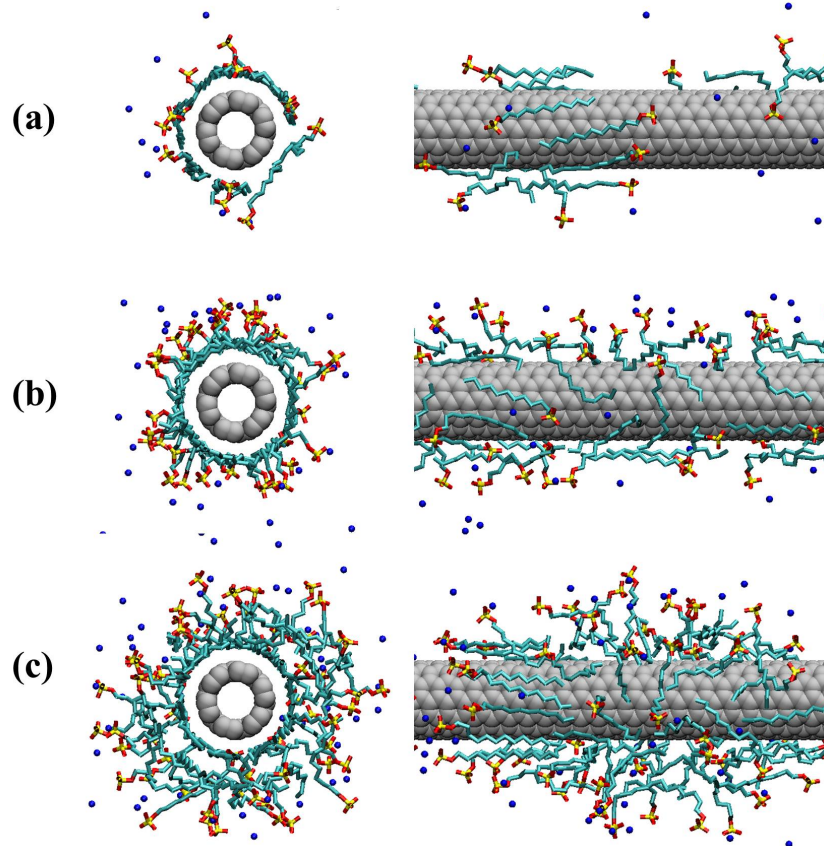


Figure S1. Front and side views of representative simulation snapshots for SDS surfactant aggregates adsorbed on (6,6) SWCNTs. In panels (a), (b), and (c) the nominal surface area per surfactant headgroup is 0.98, 0.44, and 0.25 nm^2 , respectively. Water molecules are not shown for clarity. Blue spheres are Na^+ ions. Cyan spheres are either CH_2 or CH_3 groups in the surfactant tails. Red and yellow spheres are oxygen and sulfur atoms in the surfactant headgroups.

At surfactant surface coverage of $0.98\text{ nm}^2/\text{headgroup}$, SDS molecules wrap around the nanotube forming a ring. Some surfactant headgroups are positioned close to the hydrophobic SWCNT surface [Figure S1 (a)]. As the surface coverage increases, SDS surfactants form one layer structure and the surfactant heads protrude into the aqueous solution [Figure S1 (b)]. We found bi-layered surfactant aggregates at the highest surfactant surface coverage considered ($0.25\text{ nm}^2/\text{headgroup}$). SDS surfactants were found to yield a continuous first layer at contact with the nanotube surface with excess SDS molecules agglomerate on top of the first layer yielding double-layered structures [Figure S1 (c)]. Note that this behavior is slightly different, albeit consistent, compared to that discussed in our previous work.³⁸ The multi-layered structures observed before were probably due to local minima in the free-energy landscape.

4. Effective Surface Area per Surfactant Headgroup

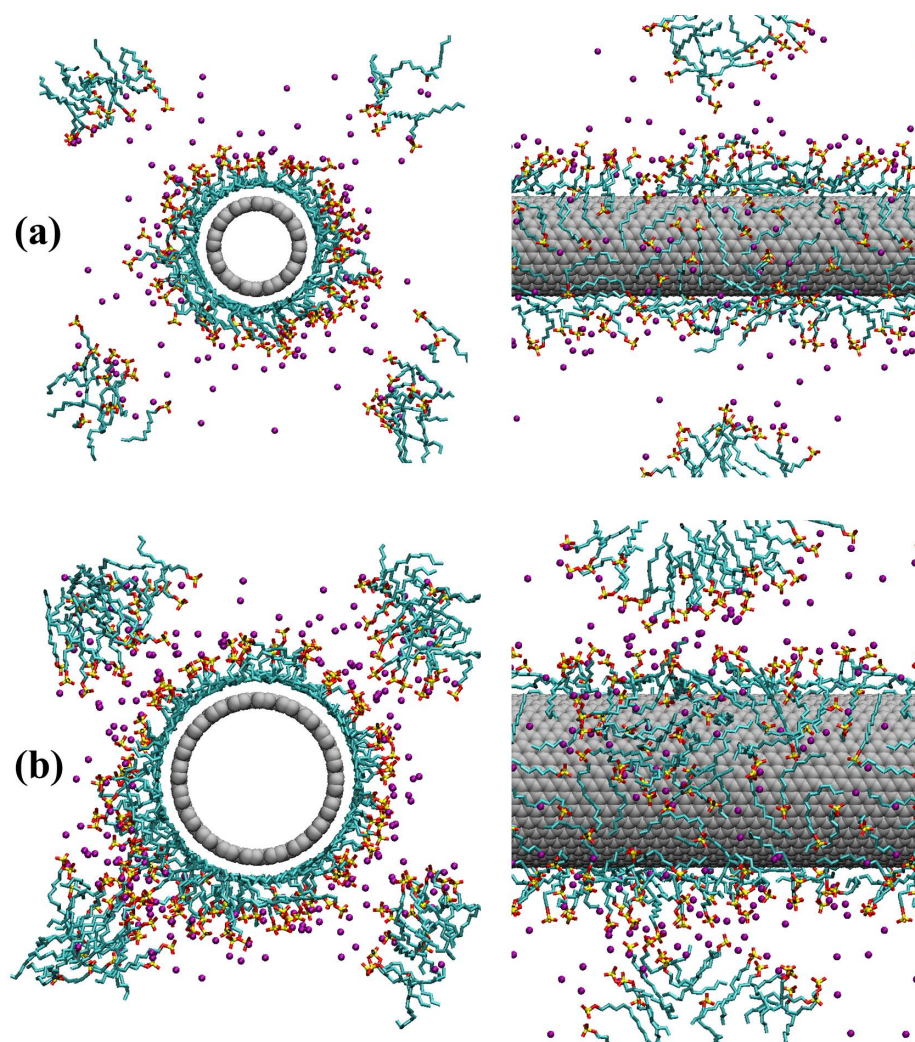


Figure S2. Front and side views of representative simulation snapshots for CsDS surfactant aggregates adsorbed on SWCNTs. The nominal surface area per surfactant headgroup is 0.25 nm^2 . Panels (a) and (b) are for (12,12) and (20,20) SWCNTs, respectively. Water molecules are not shown for clarity. Purple spheres are Cs^+ ions. Cyan spheres are either CH_2 or CH_3 groups in the surfactant tails. Red and yellow spheres are oxygen and sulfur atoms in the surfactant headgroups.

As discussed in the main text, at the highest surface coverage considered, $0.25 \text{ nm}^2/\text{headgroup}$, we observed a compact monolayer of CsDS surfactants wrapped around the three SWCNTs. The tail segments are positioned near the nanotube surface resulting from hydrophobic attractions. Most of the surfactant headgroups project into water. Details regarding the aggregate morphology are dependent on the nanotube diameter. On the (6,6) SWCNTs, all CsDS surfactants remained densely adsorbed on the nanotubes, and SDS surfactants yield rather

disordered multilayered structures. When (12,12) and (20,20) SWCNTs were simulated, some of the surfactants initially in contact with the nanotubes desorbed yielding small aggregates, in the aqueous phase when the nominal surfactant surface density was of $0.25 \text{ nm}^2/\text{headgroup}$. When the nominal surface density was of $0.44 \text{ nm}^2/\text{headgroup}$, a few surfactants desorbed and formed aggregates, but only in the case of (20,20) SWCNTs. This behavior was also observed for SDS surfactant systems at similar coverages.

We quantified the effective surface coverages of either CsDS or SDS surfactants on (12,12) and (20,20) SWCNTs at the surface coverages of 0.44 and $0.25 \text{ nm}^2/\text{headgroup}$. We calculated the time-average number of surfactants adsorbed on the SWCNT by integrating the number density profiles of the surfactant molecules around the SWCNT to a cutoff distance of 10 Å. The results are summarized in Table S2.

Table S2. Effective surfactant surface coverage for CsDS and SDS on SWCNTs.

Surfactant	SWCNT	Number of Surfactants	Nominal surfactant surface coverage ($\text{nm}^2/\text{headgroup}$)	Average number of adsorbed surfactants	Average number of non-adsorbed surfactants	Effective surfactant surface coverage ($\text{nm}^2/\text{headgroup}$)
CsDS	(12,12)	71	0.44	71	0	0.44
	(20,20)	119	0.44	82	37	0.64
	(12,12)	126	0.25	86	40	0.37
	(20,20)	210	0.25	124	86	0.42
SDS	(12,12)	71	0.44	71	0	0.44
	(20,20)	119	0.44	85	34	0.62
	(12,12)	126	0.25	90	36	0.35
	(20,20)	210	0.25	125	85	0.42

5. Radial Density Profiles on (12,12) and (20,20) SWCNTs

Density distributions of tail segments, surfactant headgroups, and counter-ions for CsDS and SDS surfactants on (12,12) and (20,20) SWCNTs at nominal surface areas of 0.44 and 0.25 nm^2 per headgroup are shown in Figure S3 and S4, respectively. The results obtained for CsDS are similar to those obtained for SDS.

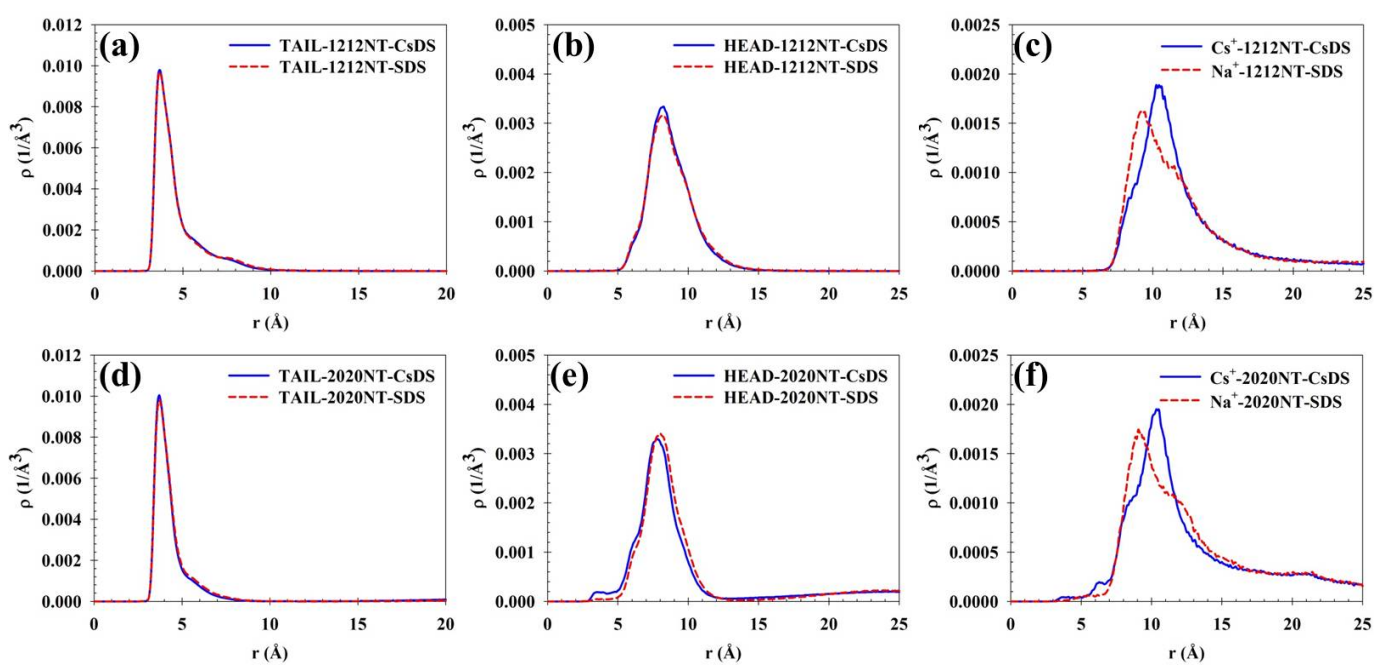


Figure S3. Radial density distributions of tail segments (left panels), surfactant headgroups (center panels), and counter-ions (right panels) obtained on (12,12) (top panels) and (20,20) SWCNTs (bottom panels). The nominal surface area per surfactant headgroup is 0.44 nm^2 . Blue solid and red dashed lines represent results obtained for CsDS and SDS systems, respectively.

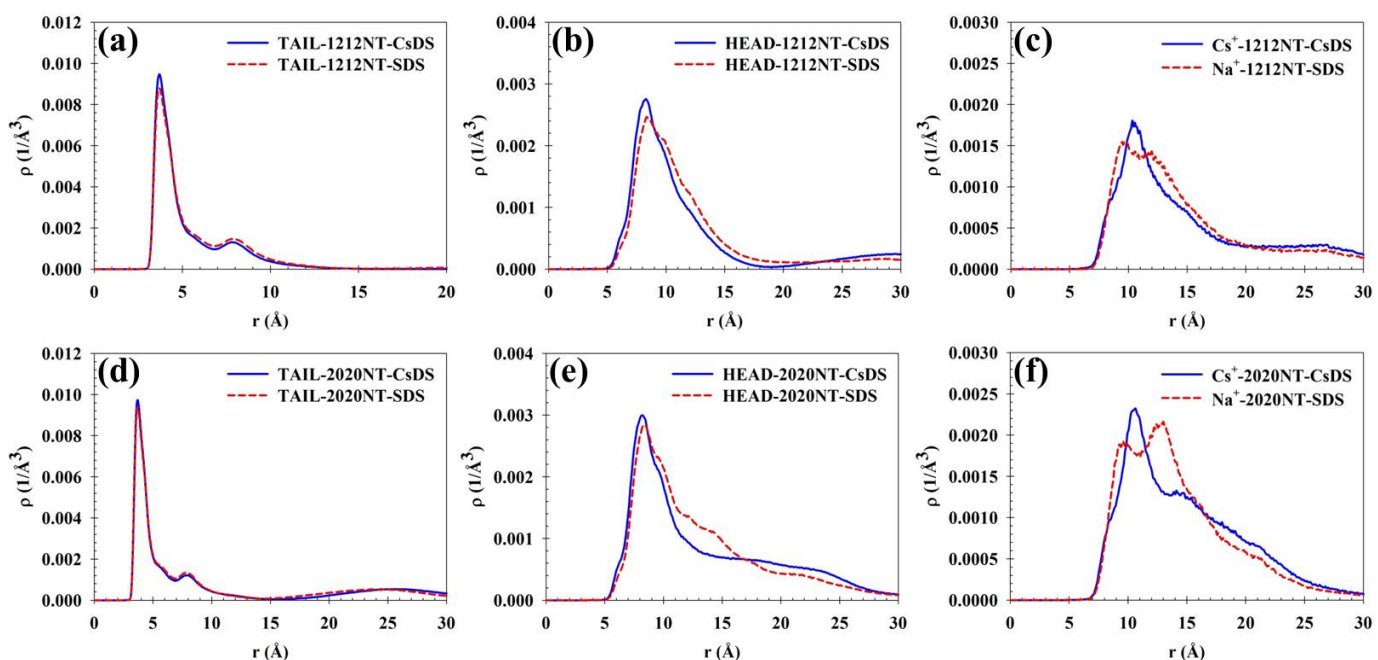


Figure S4. Same as Figure S3, but for nominal surface area per surfactant headgroup of 0.25 nm^2 .

6. Orientation of Adsorbed CsDS Surfactants

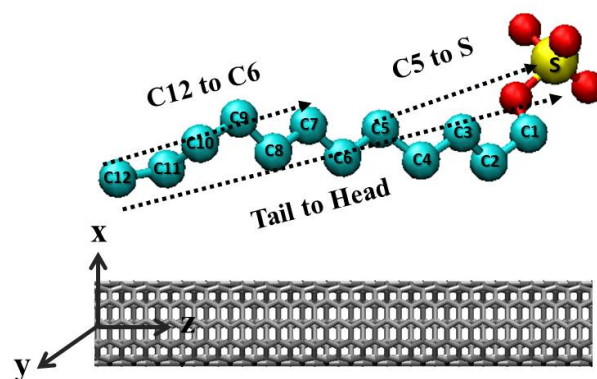


Figure S5. Schematic representing the three vectors identified by one surfactant molecule that are used to study the surfactant orientation on the nanotubes. For each surfactant we identify the tail-to-head vector, the C12-to-C6 vector in the tail, and the C5-to-S vector.

To quantify the orientations both of CsDS and of SDS adsorbed on (6,6), (12,12), and (20,20) SWCNT surfaces, we calculated the probability distribution of the angle between three vectors identified by one surfactant molecule and the SWCNT axis. The three vectors considered are the tail-to-head vector, indicative of the overall orientation of the whole surfactant with respect to the carbon nanotube, the C12-to-C6 vector, indicative of the orientation of the surfactant hydrophobic tail, and the C5-to-S vector, which can be used to qualitatively understand how much the surfactant headgroup protrudes into the aqueous phase. We provide a schematic for the three vectors in Figure S5. Note that when the angle between one of the three vectors and the SWCNT axis is 0° or 180° , the vector is parallel to the nanotube axis, while when the angle is 90° , the vector is perpendicular to the nanotube axis.

The orientation distributions for CsDS and SDS molecules on (6,6) SWCNTs at various surface coverages are shown in Figure S6. For these calculations we considered only the surfactants adsorbed at contact with the nanotube surface (as defined by the radial cutoff distance 10 Å). The orientation distribution strongly depends on the surface coverage. At low surface coverage (top panels), both CsDS and SDS surfactants preferentially lie parallel to the nanotube axis. Cs^+ counter-ions induce an orientation less parallel to the nanotube surface, which is particularly evident in the results of Figure S6 (c) (C5-to-S vector). As the surface coverage increases (middle and bottom panels), CsDS surfactants tend to yield more disordered structures compared to SDS ones (the angles distributions are much more distributed). The surfactant headgroups are much more pronouncedly projected towards the aqueous phase in the presence of Cs^+ than in the presence of Na^+ (see the preferential orientation centered around 90° for blue as opposed to red lines in Figures S6 (f) and (i)). In all cases, SDS surfactants preferentially lie parallel to the SWCNT axis.

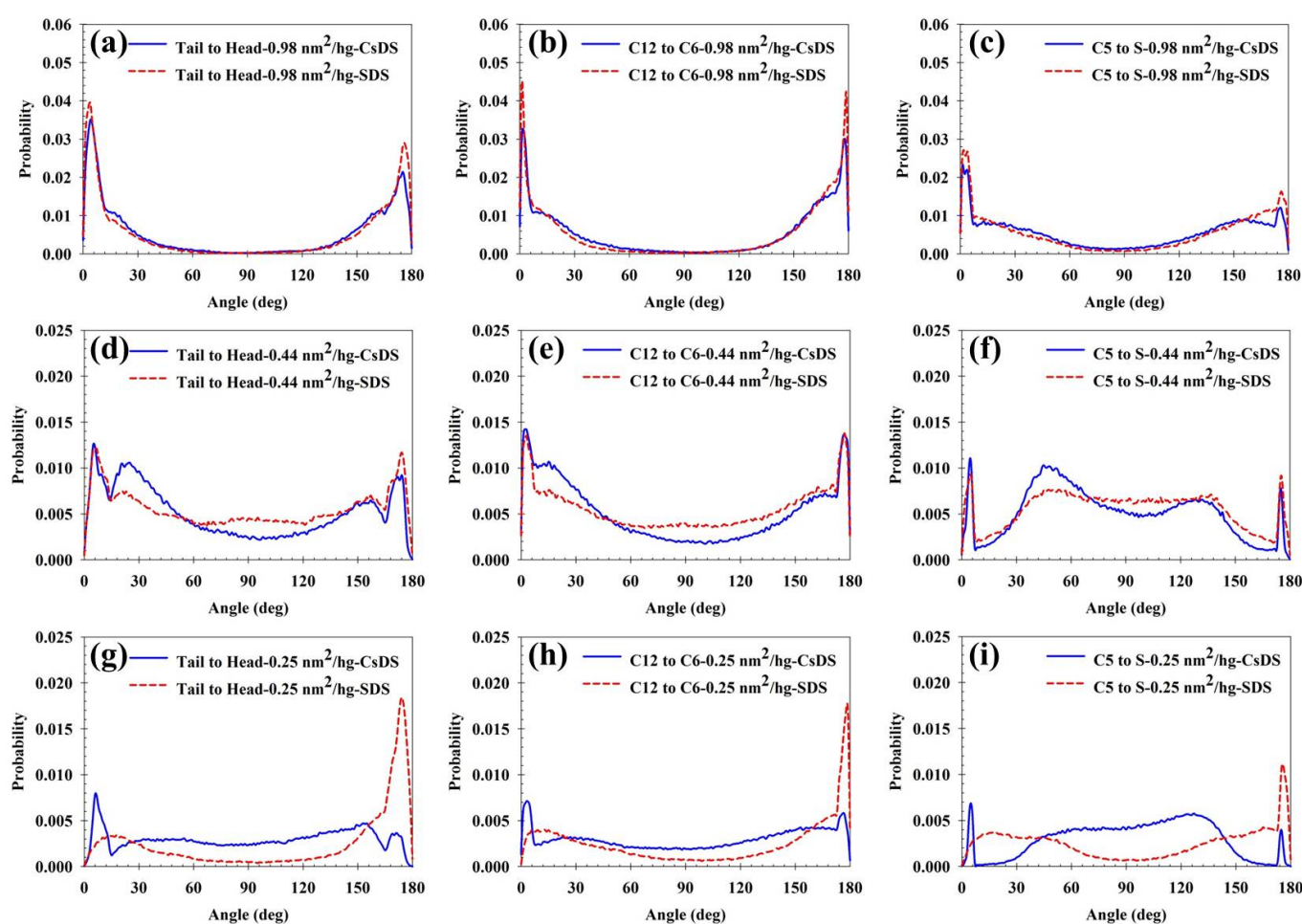


Figure S6. Orientation probability distributions observed for CsDS (blue solid) and SDS (red dashed) surfactants on (6,6) SWCNTs. Left, middle, and right panels are for the angle formed between the surfactant head-to-tail vector, that formed between the C1-to-C7 vector, and that formed between the C8-to-head vector and the nanotube axis, respectively. Top, middle, and bottom panels are for results obtained for nominal surface coverages of 0.98, 0.44, and 0.25 nm²/headgroup, respectively.

The orientation distributions for CsDS and SDS molecules on (12,12) and (20,20) SWCNTs at nominal surface coverages of 0.44 and 0.25 nm²/headgroup are shown in Figures S7 and S8, respectively. Note that only adsorbed surfactants were considered for these calculations. One surfactant was considered adsorbed if found within the radial cutoff distance of 10 Å from the nanotube surface. No significant differences were observed when the Na⁺ ions were replaced with Cs⁺ ones, in agreement with other results discussed above.

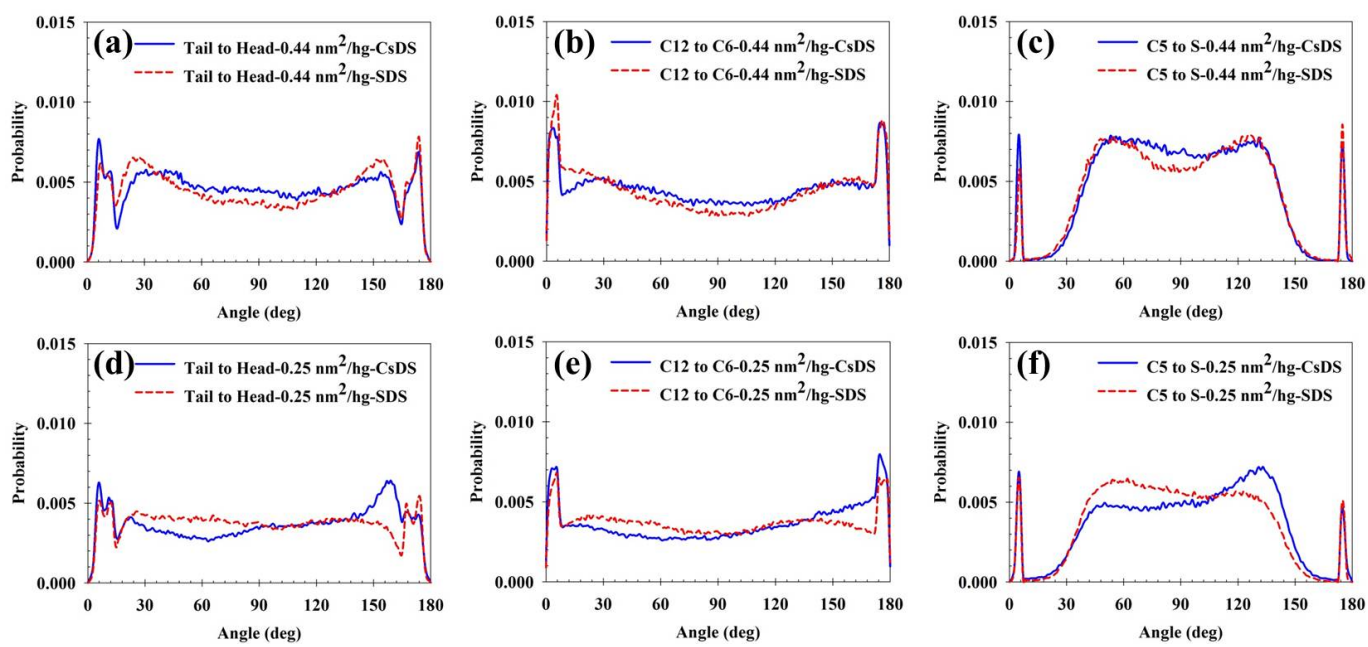


Figure S7. Orientation probability distributions observed for CsDS (blue solid) and SDS (red dashed) surfactants on (12,12) SWCNTs. Left, middle, and right panels are for the angle formed between the surfactant tail-to-head vector, that formed between the C12-to-C6 vector, and that formed between the C5-to-S vector and the nanotube axis, respectively. Top and bottom panels are for results obtained for nominal surface coverages of 0.44 and $0.25 \text{ nm}^2/\text{headgroup}$, respectively.

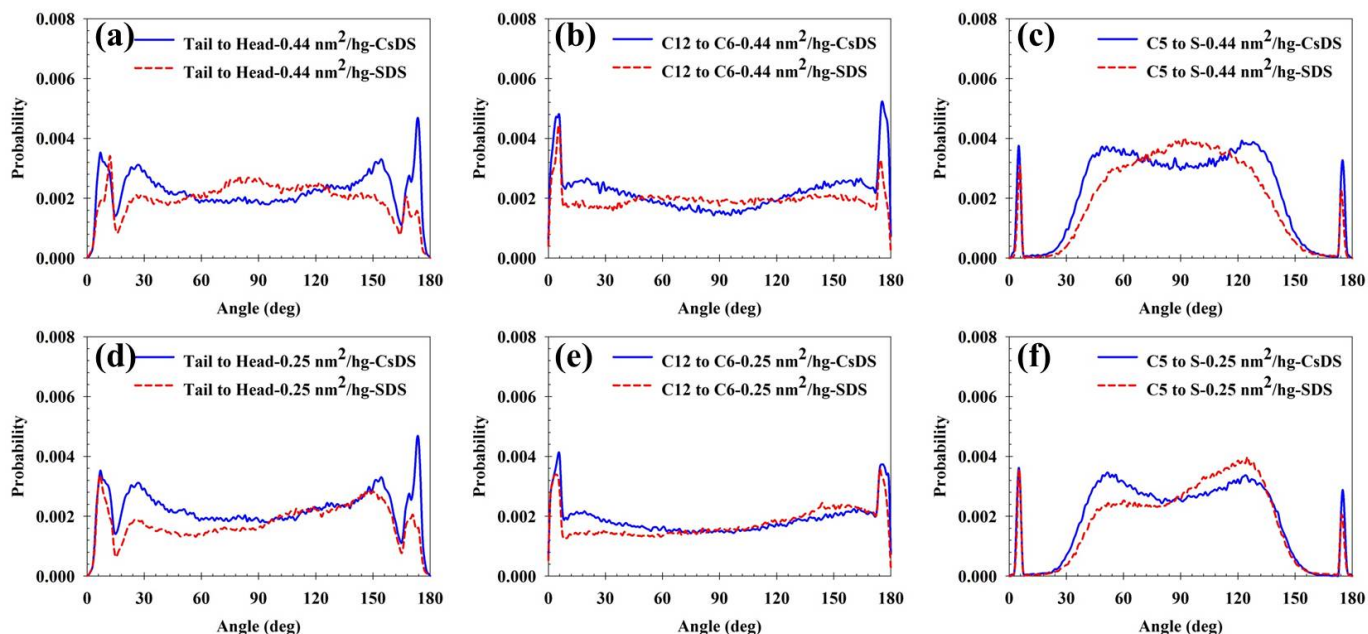


Figure S8. Same as Figure S7, but for (20,20) SWCNTs.

7. References

1. B. Hess, C. Kutzner, D. van der Spoel and E. Lindahl, *J. Chem. Theory Comput.*, 2008, **4**, 435–447.
2. A. Cheng and W. A. Steele, *J. Chem. Phys.*, 1990, **92**, 3867–3873.
3. H. J. C. Berendsen, J. R. Grigera and T. P. Straatsma, *J. Phys. Chem.*, 1987, **91**, 6269–6271.
4. D. E. Smith and L. X. Dang, *J. Chem. Phys.*, 1994, **101**, 7873 – 7881.
5. R. W. Hockney, S. P. Goel and J. W. Eastwood, *J. Comput. Phys.*, 1974, **14**, 148–158.
6. W. G. Hoover, *Phys. Rev. A: At., Mol., Opt. Phys.*, 1985, **31**, 1695–1697.
7. U. Essmann, *J. Chem. Phys.*, 1995, **103**, 8577.